

Active-Passive Seismic Isolation System for Monocrystal Pullers

Hironori FURUKAWA¹ Takafumi FUJITA² Takayoshi KAMADA³ and Hideaki MISOKA³

¹ *Yacmo Co., Ltd., Tokyo, Japan*
Email: furukawa@yacmo.co.jp

² *Institute of Industrial Science, The University of Tokyo, Japan*

³ *Tokyo University of Agriculture and Technology, Japan*

ABSTRACT :

This paper describes a seismic isolation system for monocrystal pullers. In a monocrystal puller, a monocrystal is suspended by a wire through an extremely narrow neck, and it grows longitudinally. The neck is easily broken due to the collision between the monocrystal and the wall of the puller; moreover, the regular growth of the monocrystal is stunted even during weak earthquakes. Currently, passive isolation devices are used for preventing equipment malfunctions due to earthquakes. However, in the case of the monocrystal puller, the monocrystal and wire form a pendulum with a considerably long time period. Passive isolation systems cannot sufficiently reduce the response of the pendulum to earthquakes because they may cause the pendulum to resonate. Therefore, an active isolation system is required. In this study, such a system using an AC servomotor was developed. Through shake table tests, it was demonstrated that this system could effectively reduce the displacement of the monocrystal model.

KEYWORDS: Seismic Isolation, Active Isolation, Monocrystal Puller, Linear Motor, Simulation Analysis

1. INTRODUCTION:

In order to manufacture silicon monocrystals, approximately 90% of the monocrystals are grown by the Czochralski (CZ) method. In this process, the seed crystal is immersed in the melting silicon and then withdrawn slowly. A monocrystal forms at the end of the seed crystal and it grows longitudinally as it is withdrawn (shown in Figure 1). The monocrystal is suspended by a wire through an extremely narrow neck that is easily broken when subjected to shocks. Moreover, the regular growth of the monocrystal is stunted even during weak earthquakes. Currently, passive isolation devices are used for preventing equipment malfunctions due to earthquakes. However, in the case of a monocrystal puller, the monocrystal and wire form a pendulum with a long time period; therefore, the pendulum may be made to resonate by employing passive isolation devices. In this study, an active isolation system using AC servomotors is developed.

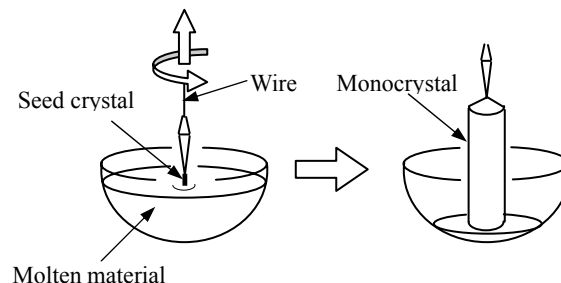


Figure 1 Growth of a monocrystal (CZ method)

2. MONOCRYSTAL PULLER MODEL AND ACTIVE ISOLATION DEVICE:

The movable frame of the isolation device is supported by four linear bearings and it is connected to the base frame by a tension spring and a viscous damper. The AC servomotor is fixed on the base frame, and the output shaft of its motor is connected to the ball screw with a coupling. The mobile flange, which is a part of the ball

screw, is connected to the movable frame. The natural frequency of the isolation device is approximately 0.25 Hz. The monocrystal model is in the form of a pillar and has a mass of 63 kg, that is suspended from the top of the monocrystal puller model by a wire cable. The natural frequency of the pendulum formed by the wire cable and the monocrystal model is approximately 0.4 Hz (Figure 2).



Figure 2 Image of the experimental model

3. CONTROL SYSTEM:

The control system is shown in Figure 3. The acceleration signal detected by the sensor attached to the isolation device is sent to the digital signal processor (DSP) through the A/D converter. Subsequently, the command voltage is calculated according to the algorithm designed beforehand and input into the motor driver through the D/A converter. In the driver, the optimal current value for driving the AC servomotor is computed on the basis of the inputted command voltage, and this current is then supplied to the AC servomotor.

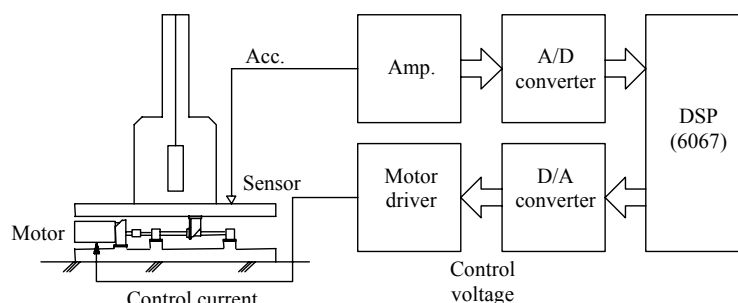


Figure 3 Control system

4. ANALYTICAL MODEL:

4.1. 3-mass/4-degrees-of-freedom system model

The analytical model of the monocrystal puller model and isolation device is shown in Figure 4. In this study, the system is considered to be a 3-mass/4-degrees-of-freedom system comprising the isolation device, monocrystal puller model, and monocrystal model.

The slide part of isolation device has friction. Therefore, the state of device is divided into fixation and an operation by the size of an input seismic wave. Here, an equation of motion is as follows, when that a fixation state is Phase1 and an operation state is Phase2.

Phase 1: The case wherein the isolation device is fixed by employing the friction acting on the sliding part of the system.

$$\ddot{x}_2 + \ddot{z} = -\frac{c_2}{m_2} \dot{x}_2 + \frac{k_2}{m_2} x_1 - \frac{k_2}{m_2} x_2 + \frac{c_{\theta 1} + c_{\theta 2}}{m_2 l_1} \dot{\theta}_1 - \frac{c_{\theta 2}}{m_2 l_1} \dot{\theta}_2 + \frac{m_3 g}{m_2} \theta_1 \quad (1)$$

$$\ddot{\theta}_1 = \frac{c_2}{m_2 l_1} \dot{x}_2 - \frac{k_2}{m_2 l_1} x_1 + \frac{k_2}{m_2 l_1} x_2 - \left\{ \left(\frac{1}{m_2 l_1^2} + \frac{l_2^2}{4 l_1^2 I_c} + \frac{1}{m_3 l_1^2} \right) (c_{\theta 1} + c_{\theta 2}) + \frac{l_2}{2 l_1 I_c} c_{\theta 2} \right\} \dot{\theta}_1$$

$$+ \left(\frac{1}{m_1 l_1^2} + \frac{l_2^2}{4 l_1^2 I_c} + \frac{l_2}{2 l_1 I_c} + \frac{1}{m_3 l_1^2} \right) c_{\theta 2} \cdot \dot{\theta}_2 - \left(\frac{m_3 g}{m_1 l_1} + \frac{m_3 l_2^2 g}{4 l_1 I_c} + \frac{g}{l_1} \right) \theta_1 + \frac{m_3 l_2^2 g}{4 l_1 I_c} \theta_2 - \frac{1}{m_3 l_1} \text{sign}(\dot{x}_c - x_1) f_{cr} \quad (2)$$

$$\ddot{\theta}_2 = \left(\frac{l_2}{l_1} \cdot \frac{c_{\theta 1} + c_{\theta 2}}{2 I_c} + \frac{c_{\theta 2}}{I_c} \right) \dot{\theta}_1 - \left(\frac{l_2}{l_1} \cdot \frac{c_{\theta 2}}{2 I_c} + \frac{c_{\theta 2}}{I_c} \right) \dot{\theta}_2 + \frac{m_3 l_2 g}{2 I_c} \theta_1 - \frac{m_3 l_2 g}{2 I_c} \theta_2 \quad (3)$$

Phase 2: The case wherein the isolation device is in operation.

$$\ddot{x}_1 + \ddot{z} = -\frac{c_1 + c_2}{m_1} \dot{x}_1 + \frac{c_2}{m_1} \dot{x}_2 - \frac{k_1 + k_2}{m_1} x_1 + \frac{k_2}{m_1} x_2 + \frac{1}{m_1} (u + \text{sign}(\dot{x}_c - \dot{x}_1) f_{cr} - \text{sign}(\dot{x}_1) \mu (m_1 + m_2 + m_3) g) \quad (4)$$

$$\ddot{x}_2 + \ddot{z} = \frac{c_2}{m_2} \dot{x}_1 - \frac{c_2}{m_2} \dot{x}_2 + \frac{k_2}{m_2} x_1 - \frac{k_2}{m_2} x_2 + \frac{c_{\theta 1} + c_{\theta 2}}{m_2 l_1} \dot{\theta}_1 - \frac{c_{\theta 2}}{m_2 l_1} \dot{\theta}_2 + \frac{m_3 g}{m_2} \theta_1 \quad (5)$$

$$\ddot{\theta}_1 = -\frac{c_2}{m_2 l_1} \dot{x}_1 + \frac{c_2}{m_2 l_1} \dot{x}_2 - \frac{k_2}{m_2 l_1} x_1 + \frac{k_2}{m_2 l_1} x_2 - \left\{ \left(\frac{1}{m_2 l_1^2} + \frac{l_2^2}{4 l_1^2 I_c} + \frac{1}{m_3 l_1^2} \right) (c_{\theta 1} + c_{\theta 2}) + \frac{l_2}{2 l_1 I_c} c_{\theta 2} \right\} \dot{\theta}_1$$

$$+ \left(\frac{1}{m_1 l_1^2} + \frac{l_2^2}{4 l_1^2 I_c} + \frac{l_2}{2 l_1 I_c} + \frac{1}{m_3 l_1^2} \right) c_{\theta 2} \cdot \dot{\theta}_2 - \left(\frac{m_3 g}{m_1 l_1} + \frac{m_3 l_2^2 g}{4 l_1 I_c} + \frac{g}{l_1} \right) \theta_1 + \frac{m_3 l_2^2 g}{4 l_1 I_c} \theta_2 - \frac{1}{m_3 l_1} \text{sign}(\dot{x}_c - x_1) f_{cr} \quad (6)$$

$$\ddot{\theta}_2 = \left(\frac{l_2}{l_1} \cdot \frac{c_{\theta 1} + c_{\theta 2}}{2 I_c} + \frac{c_{\theta 2}}{I_c} \right) \dot{\theta}_1 - \left(\frac{l_2}{l_1} \cdot \frac{c_{\theta 2}}{2 I_c} + \frac{c_{\theta 2}}{I_c} \right) \dot{\theta}_2 + \frac{m_3 l_2 g}{2 I_c} \theta_1 - \frac{m_3 l_2 g}{2 I_c} \theta_2 \quad (7)$$

The conditions for phase change are as follows.

○ Phase 1 → Phase 2:

$$|m_1 \ddot{z} - c_2 \dot{x}_2 + (k_1 + k_2) x_1 - k_2 x_2 - u - f_{cr}| > \mu (m_1 + m_2 + m_3) g \quad (8)$$

○ Phase 2 → Phase 1:

$$\dot{x}_1 = 0 \quad \text{and} \quad |m_1 (\ddot{x}_1 + \ddot{z}) - c_2 \dot{x}_2 + (k_1 + k_2) x_1 - k_2 x_2 - u - f_{cr}| \leq \mu (m_1 + m_2 + m_3) g \quad (9)$$

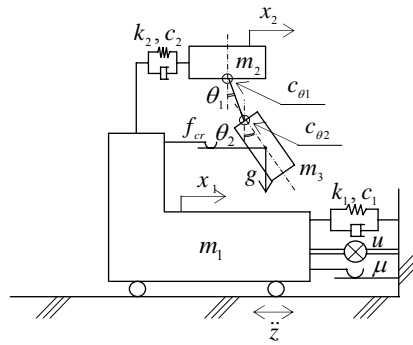


Figure 4 Analytical model

5. CONTROL DESIGN:

5.1. The dynamic characteristic of the AC servomotor

Here, T_M , η_M , l , and η_B represent the rated torque of the AC servomotor, efficiency of the motor, lead pitch of the ball screw, and efficiency of the ball screw, respectively; the force generated, F , is expressed as follows:

$$F = \frac{T_M \cdot 2\pi \cdot \eta_M \cdot \eta_B}{l} = 1566.8 [N] \quad (10)$$

This force is generated by the command signal whose voltage is 3.33 V.

Hence,

$$F_a = \frac{1566.8}{3.33} = 470 [N/V] \quad (11)$$

The dynamic characteristic of the operation system is assumed to have a constant F_a value.

5.2. 1-mass system model for control design

Since a silicon monocrystal is in a high-temperature state at 1400°C in a monocrystal puller and since it rotates continuously during the production process, it is particularly difficult to obtain direct measurements. Hence, the controller was built to operate with the acceleration data of only the isolation device. Therefore, the movement model for the control system design is a 1-mass system, as shown in Figure 5.

$$m_1 \ddot{x}_1 + \tilde{c}_1 \dot{x}_1 + k_1 x_1 = F_a - m_1 \ddot{z} \quad (12)$$

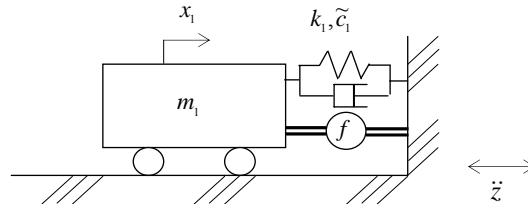


Figure 5 Analytical model for the control system design

5.3. Model-matching method

In this study, the controller was designed by using the model-matching method. As a reference, this method constructs a closed loop transfer function based on the transfer function of a plant for visual comprehension, and it then builds the control system that achieves the closed loop transfer function through a reverse operation. Here, the system shown in Figure 6 is considered.

When this system is set with $y = L(\ddot{x} + \ddot{z})$, $u = L(u)$, $d = L(\ddot{z})$, y is expressed as follows:

$$y = P_{uy} \cdot u + P_{dy} \cdot d \quad (13)$$

Here, P_{uy} is an open loop transfer function from a control input to an output and P_{dy} is the disturbance to the plant. Moreover, when C_{yu} is converted into an open loop transfer function from an output to a control input and C_{ru} is converted into the target value of a controller, W_{ry} , W_{vy} , and, W_{dy} that indicate the target value, observation noise, and the closed loop transfer function from the disturbance to an output are expressed as follows:

$$W_{ry} = (1 - P_{uy} C_{yu})^{-1} P_{uy} C_{ru} \quad (14)$$

$$W_{vy} = (1 - P_{uy} C_{yu})^{-1} P_{uy} C_{yu} \quad (15)$$

$$W_{dy} = (1 - P_{uy} C_{yu})^{-1} P_{dy} \quad (16)$$

To ensure a satisfactory controller design by the model-matching method, W_{ry} and W_{vy} must satisfy the following three conditions.

(1) Realization conditions

The relative degrees of W_{ry} and W_{vy} are larger than the relative degree of P_{uy} .

(2) Connection conditions

The zero points of W_{ry} and W_{vy} contain all the zero points of P_{uy} .

(3) Degree conditions

The zero points of $(1 + W_{vy})$ contain all the poles of P_{uy} .

Furthermore, it is possible to include the filter characteristic in a controller by providing the dynamic characteristics. The controller is designed by specifying the transfer function W_{dy} from the disturbance to an output.

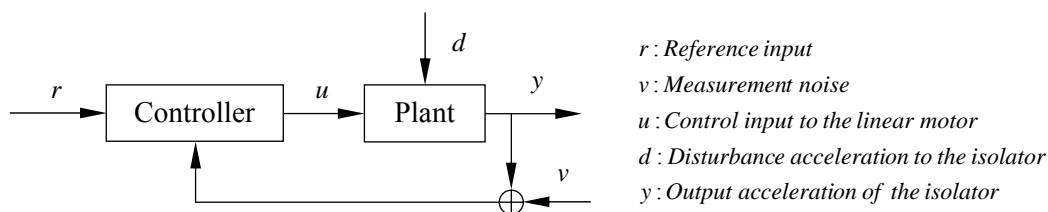


Figure 6 Block diagram of control system

5.4. Determination of parameters of a controller

The controller is designed by determining the system-wide poles; W_{dy} is shown in Figure 7.

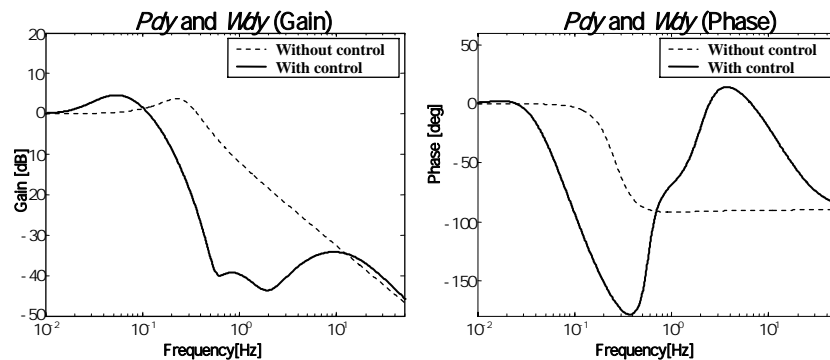


Figure 7 W_{dy}

6. EXPERIMENTAL RESULTS:

6.1. Shaking table tests

In the excitation tests, the earthquake input was the ground motion records for the El Centro wave (Imperial Valley Earthquake, 1940). The peak accelerations of the earthquake input was adjusted to 0.1 and 0.5 m/s^2 . Figures 8-11 shows the time history displacements of the monocystal model and the acceleration transmissibility from the shake table to the movable frame. The examination of the amplitudes of the monocystal model reveals that passive isolation cannot reduce the displacement of the monocystal model because the natural frequency of the isolation device is not sufficiently low as compared to that of a pendulum. Therefore, passive isolation provides only limited protection to a monocystal. On the other hand, active isolation effectively reduces the displacement of the monocystal model.

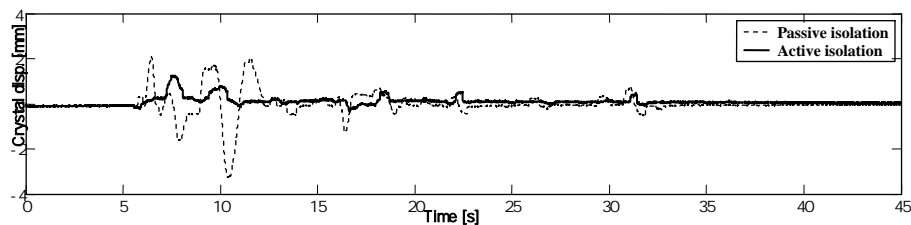


Figure 8 Experimental results (Displacement of the monocystal [Input =El Centro NS 0.1 m/s^2])

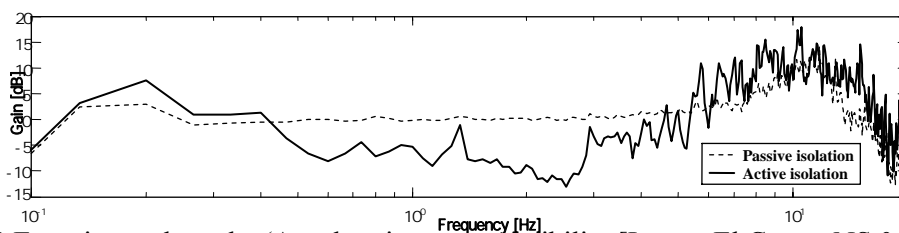


Figure 9 Experimental results (Acceleration transmissibility [Input =El Centro NS 0.1 m/s^2])

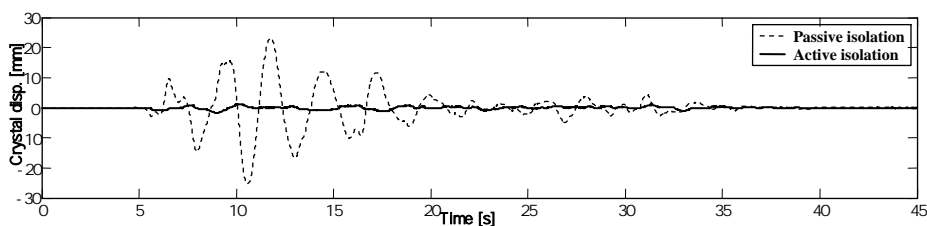


Figure 10 Experimental results (Displacement of the monocystal [Input = El Centro NS 0.5 m/s^2])

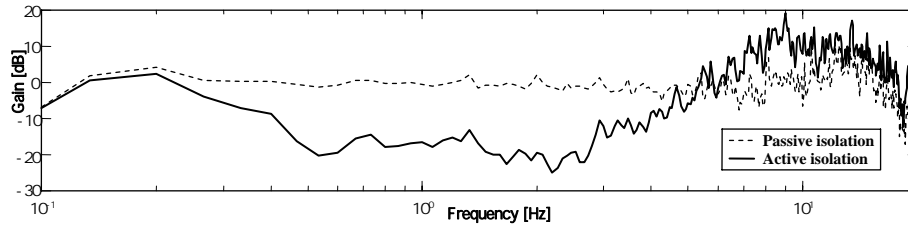


Figure 11 Experimental results (Acceleration transmissibility [Input = El Centro NS 0.5 m/s²])

6.2. Robustness

In the monocrystal puller, the natural frequency of the pendulum, which comprises a monocrystal and wire, changes as the wire pulls up the monocrystal. Therefore, the designed controller must be sufficiently robust so that the seismic isolation performance does not degrade even when the dynamic characteristic of the pendulum changes. The adjustment of the wire length in three stages approximates the changes in the dynamic characteristic of the pendulum accompanying the monocrystal withdrawal process, and the seismic isolation performance of each case is verified. The wire lengths are Len 1 (= 1425 mm) and Len 2 (= 345 mm) in the descending order.

Figure 12 show the maximum displacement of the monocrystal model when isolated by using the passive and active modes. The controller is designed for Len 1. However, by comparing the displacements of the monocrystal model when isolated by the passive and active modes, irrespective of the wire length, the performance of the controller was examined, and it was found that the displacement of the monocrystal model decreased by an amount ranging from -65% to -99%. Therefore, it can be stated that the controller designed in this study is robust with respect to changes in the wire length.

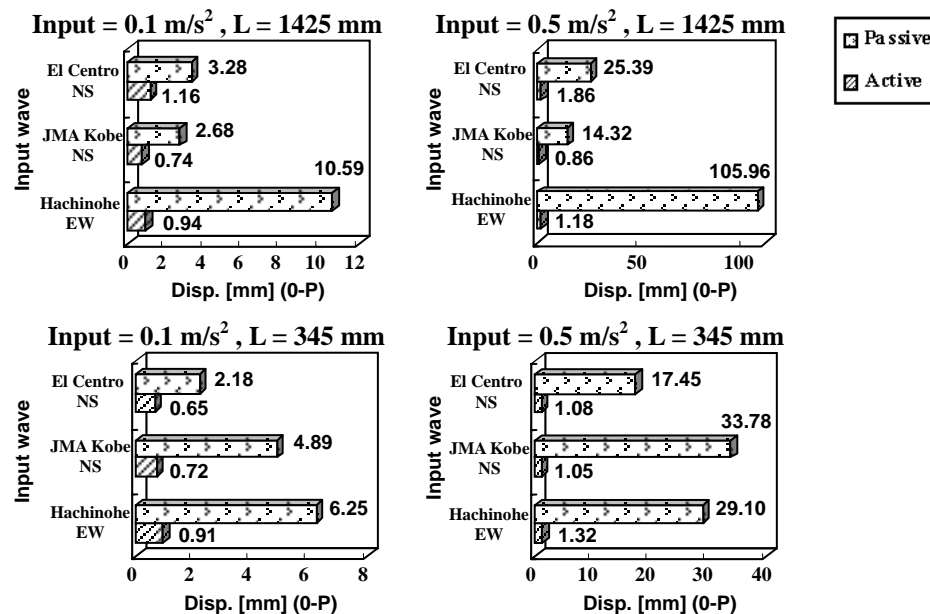


Figure 12 Maximum displacement of the monocrystal model

6.3. Active-passive modes switching tests

Evidently, when a weak earthquake occurs, the isolation system works as an active isolation device that can effectively protect the monocrystal. Furthermore, the isolation system must automatically switch to the passive mode when a strong earthquake which exceeding the capacity limit of the AC servomotor occurs. The active-passive modes switching tests were carried out in order to examine the variations in the isolation performance.

Figures 13 show the time history accelerations of the movable frame when isolated by the passive mode alone and by the hybrid mode with active-passive mode switching, respectively. The test results reveal that while switching to the passive mode, the acceleration of the movable frame exhibited a response that is equivalent to the result of the passive isolation experiment. Further, it was revealed that this switching process was performed

smoothly.

Thus, the effectiveness of active-passive mode switching was verified on the basis of the protection systems for the motor and driver.

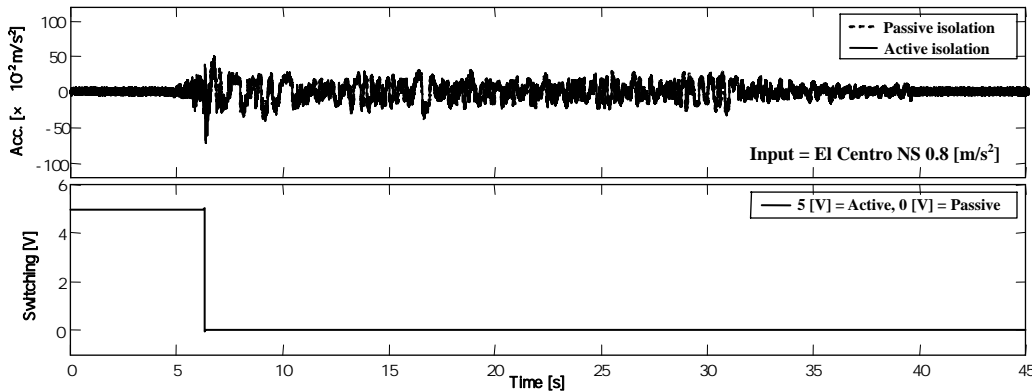


Figure 13 Excitation experiment with active-passive modes (Input = El Centro NS 0.8 m/s²)

7. SIMULATION ANALYSIS:

7.1. Comparative study by simulation

Using the derived equation, the time history displacements of the monocrystal model during isolation by the passive and active modes were simulated. The ground motion record from the El Centro wave (Imperial Valley Earthquake, 1940) was used in the simulation. The peak accelerations of the earthquake inputs were adjusted to 0.3 m/s². From the time history displacements of the monocrystal models, devices, and control voltage, the shapes of the waves obtained in the calculated results and experimental results are in good agreement (shown in Figures 14-16).

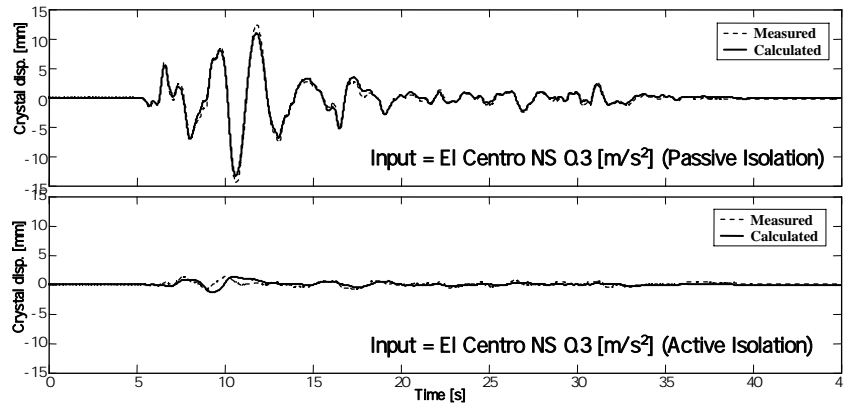


Figure 14 Simulation analysis result (Displacement of the monocrystal [Input = El Centro NS 0.3 m/s²])

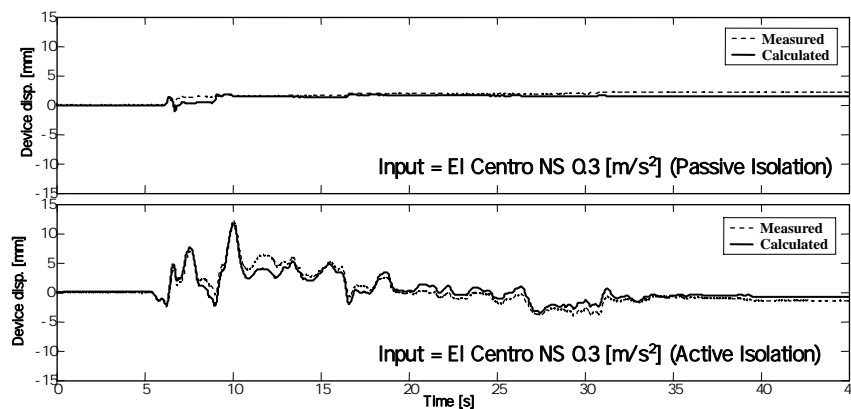


Figure 15 Simulation analysis result (Displacement of the device [Input = El Centro NS 0.3 m/s²])

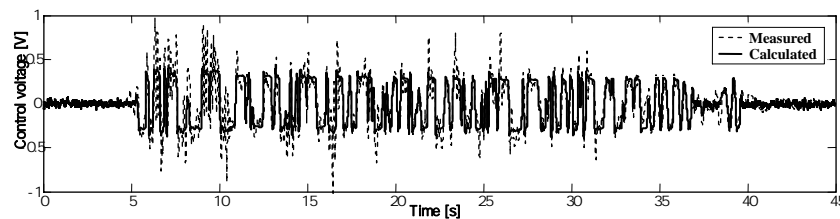


Figure 16 Simulation analysis result (Control voltage [Input = El Centro NS 0.3 m/s²])

8. CONCLUSION:

A seismic isolation system with interchangeable active and passive modes is developed using an AC servomotor. The performance of the system has been verified by the time history displacement of the monocystal model. The conclusions can be summarized as follows:

- (1) The use of an AC servomotor in the active isolation system is effective in preventing the collisions of the monocystal resulting from earthquakes.
- (2) It was confirmed that the active isolation system using a controller designed by the model-matching method reduces the displacement of the monocystal.
- (3) The effectiveness of the active-passive mode switching was examined on the basis of the protection systems for the motor and driver.
- (4) It was possible to simulate the response of the monocystal to an earthquake almost accurately by using the analysis program.

REFERENCES

1. T. Fujita, Q. Feng, E. Takenaka, T. Takano, and Y. Suizu, "Active Isolation of Sensitive Equipment for Weak Earthquakes," Proceeding of Ninth World Conference on Earthquake Engineering, Vol.8, SE-10 (1988).
2. T. Fujita, Y. Tagawa, N. Murai, S. Shibuya, A. Takeshita, and Y. Takahashi, "Study of Active Microvibration Control Device Using Piezoelectric Actuator (1st Report, Fundamental Study of One-Dimensional Microvibration Control)," Trans. of the Japan Society of Mechanical Engineers, Vol.57, No.540, Ser. C, (in Japanese) (1991).
3. T. Fujita, K. Tanaka, H. Ohyama, Y. Nakamura, H. Hora, H. Miyano, and M. Suganuma, "Large-Scale Model Experiment of Hybrid Mass Damper with Convertible Active and Passive Modes Using Linear Motor for Vibration Control of Tall Buildings," Trans. of the Japan Society of Mechanical Engineers, Vol.62, No.594, Ser. C, (in Japanese) (1996).
4. H. Furukawa, T. Fujita, T. Kamada, and H. Misoka "Experimental and Analytical Studies of Active-Passive Seismic Isolation System Using Linear Motors for Monocystal Pullers" In: Proceedings of the 9th World Seminar on Seismic Isolation, Energy Dissipation and Active Vibration Control of Structure, Kobe, Japan (2005), Vol.□463-470.
5. H. Furukawa, T. Fujita, T. Kamada, and H. Misoka "Development of Active-Passive Seismic Isolation Using AC Servomotors for Monocystal Pullers" In: Proceedings of the 10th World Seminar on Seismic Isolation, Energy Dissipation and Active Vibration Control of Structure, Istanbul, Turkey (2007).